

Response of double hinged articulated tower platforms to wind forces

Nazrul Islam and Mohd Moonis Zaheer*

Department of Civil Engineering, Jamia Millia Islamia, New Delhi-110025, India

Suhail Ahmed

Department of Applied Mechanics, Indian Institute of Technology, Delhi-110016, India

(Received March 28, 2008, Accepted December 29, 2008)

Abstract. Articulated tower platforms due to its compliant nature are more susceptible to the dynamic effects of wind than conventional fixed platforms. Dynamic response analysis of a double hinged articulated tower excited by low frequency wind forces with random waves is presented in this paper. The exposed super structure of the platform, housing the drilling and production facilities is subjected to mean and fluctuating wind loads, while the submerged portion is acted upon by wind driven waves. The fluctuating component of the wind velocity is modeled by Emil Simiu's spectrum, while the sea state is characterized by Pierson-Moskowitz spectrum. Nonlinearities in the system due to drag force, added mass, variable submergence and instantaneous tower orientation are considered in the analysis. To account for these nonlinearities, an implicit time integration scheme (Newmark's- β) has been employed which solves the equation of motion in an iterative fashion and response time histories are obtained. The power spectra obtained from random response time histories show the significance of low frequency responses.

Keywords: offshore structures; dynamic response; articulated loading platform; wind driven waves; sea site wind spectrum; compliant tower; nonlinearities; turbulent wind.

1. Introduction

An articulated tower, as shown in Fig. 1, is one of the compliant offshore structures which are designed for deep water applications. Typically these structures are supported near the sea bed through a universal joint. The tower shaft extending through the water surface consists of a ballast chamber, a steel lattice structure, buoyancy chamber, and a chimney supporting the deck above the water surface. This type of structure is being used as an efficient means of mooring or as loading terminal for oil tankers in open waters, flare towers as well as production riser and control tower in remote offshore environment.

Although wave loading on offshore platforms is generally assumed to be more significant than wind loading, exceptions can be found. Low frequency deep water articulated towers reduce the

* Corresponding Author, E-mail: mooniszaheer@rediffmail.com

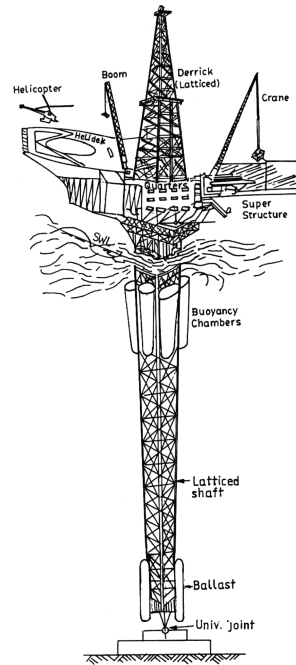


Fig. 1 Articulated tower

response to high frequency wave forces. However, the structure vibrates within range of the most energetic low frequencies of wind excitation. This places greater importance of wind action on the behaviour of articulated loading platforms.

A sample of studies dealing with the dynamic analysis of single hinged articulated towers (SHAT) under wind loading has been carried out by Deleuil and Durgiet (1987); Datta and Jain (1990); Bar-Avi and Benaroya (1997) and Ahmad and Islam (2001). Fatigue and fracture reliability of articulated joint under wind and wave environment is carried out by Islam and Ahmad (2007). In a recent paper, Zaheer and Islam (2008) carried out extensive review on aerodynamic behaviour of single and double hinged articulated towers. Literature concerning the dynamic analysis of double hinged articulated towers (DHAT) is very limited. Mc Namara and lane (1984) discusses the finite element analysis of multi-hinged articulated towers. Hanna, *et al.* (1988) gave a new concept of Tension Restrained Articulated Platform (TRAP). Their study concluded that multi articulation concept is an attractive option for deepwater applications. Helvacioğlu and Incecik (1988) gave an analysis and model test of SHAT and DHAT. Zaheer and Islam (2008) compared the responses of double hinged ALP under different wind spectra. While analytical solutions under uncorrelated wind and waves have been generally presented, responses under correlated wind and wave environment are lacking. This study provides a combined effect of wind and wave forces on the tower behaviour.

2. Assumptions

Following assumptions are made in the analysis of the tower.

1. The flexural deformations of the tower are assumed to be small as compared to its displacement as a rigid body.

2. The platform is idealized as an inverted double pendulum, displacing only in the plane of fluid loading.
3. The tower has uniform properties over the segments of uniform diameters.
4. The tower shaft is assumed to be hinged at the base and at an intermediate level.

3. Development of equations of motion

The equations of motion of DHAT are derived using Lagrange’s equation. The tower model consists of two-degree-of-freedom system, rotations θ_1 and θ_2 about the vertical axis (Fig. 2a). The generalized force is derived using the principle of conservation of energy. In the derivation of equations of motion, “1” stands for lower tower, while “2” stands for upper tower.

The general form of Lagrange’s equation is:

$$\frac{d}{dt}\left(\frac{\partial T}{\partial \dot{\theta}_i}\right) - \frac{\partial T}{\partial \theta_i} + \frac{\partial V}{\partial \theta_i} = Q_{\theta_i} \quad (1)$$

where, T , V and Q_{θ_i} represents the kinetic energy, the potential energy and the generalized force respectively.

The kinematic relationships for the double hinged tower model can be expressed as:

$$x = L_1 \sin \theta_1 + r_{2j} \sin \theta_2 \quad (2)$$

$$y = L_1 \cos \theta_1 + r_{2j} \cos \theta_2 \quad (3)$$

where L_1 = length of the bottom tower and r_{2j} = position vector of an element in the top tower. Using Eqs. (2) and (3), the resultant velocity is given by

$$V^2 = L_1^2 \dot{\theta}_1^2 + r_{2j}^2 \dot{\theta}_2^2 + 2L_1 r_{2j} \cos(\theta_2 - \theta_1) \dot{\theta}_1 \dot{\theta}_2 \quad (4)$$

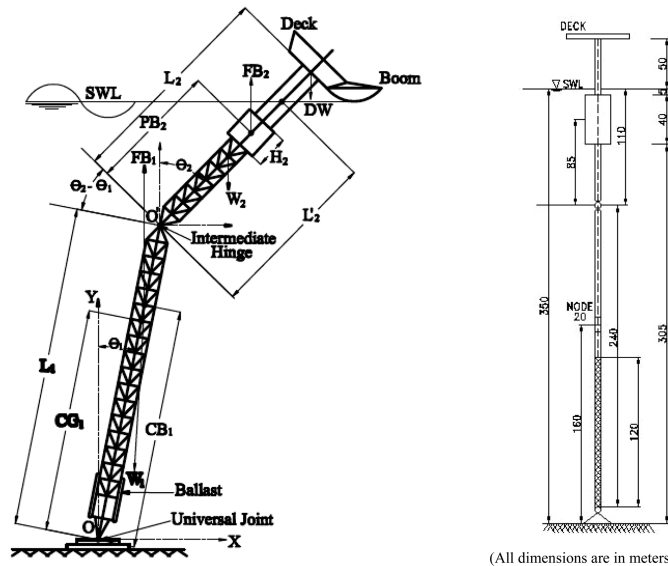


Fig. 2 (a) Mathematical model of DHAT (b) Idealized double hinged tower

3.1. Kinetic energy

The kinetic energy, T for the tower can be expressed as:

$$T = T_1 + T_2 \quad (5)$$

where T_1 , T_2 are the kinetic energies of the lower and upper towers.

$$T_1 = \frac{1}{2} \sum_{i=1}^{N_p} (m_{1i}) \cdot (r_{1i} \dot{\theta}_1)^2 = \frac{1}{2} \left[\sum_{i=1}^{N_p} (m_{1i}) r_{1i}^2 \right] \dot{\theta}_1^2 = \frac{1}{2} I_{1t} \dot{\theta}_1^2 \quad (6)$$

where m_{1i} is the mass of an element in tower “1” and r_{1i} is its position vector.

T_2 consists of three components, viz: kinetic energy of elements submerged in water (T_{2water}), kinetic energy of elements between water level and underside of deck (T_{air}) and kinetic energy of deck (T_{deck}) respectively.

The resulting kinetic energy of top tower may now be expressed as:

$$\begin{aligned} T_2 = & \frac{1}{2} \left[\sum_{j=1}^{N_w} (m_{2j}) \{ (L_1 \dot{\theta}_1)^2 + (r_{2j} \dot{\theta}_2)^2 + 2L_1 r_{2j} \cos(\theta_2 - \theta_1) \dot{\theta}_1 \dot{\theta}_2 \} \right] \\ & + \sum_{j=N_w+1}^{N_p} m_{2j} \{ (L_1 \dot{\theta}_1)^2 + (r_{2j} \dot{\theta}_2)^2 + 2L_1 r_{2j} \cos(\theta_2 - \theta_1) \dot{\theta}_1 \dot{\theta}_2 \} \\ & + m_d \{ (L_1 \dot{\theta}_1)^2 + (L_p \dot{\theta}_2)^2 + 2L_1 L_p \cos(\theta_2 - \theta_1) \dot{\theta}_1 \dot{\theta}_2 \} + \frac{1}{2} I_d \dot{\theta}_2^2 \end{aligned} \quad (7)$$

The total masses $m_{it} = (m_i + am_i)$ is used to calculate the kinetic energy of the towers account for the structural mass and the inertial added mass due to the motion of the structure; m_d is the mass of deck; I_d is the moment of inertia of deck, L_p is the height of c.g of the deck above mid hinge and N_w is the number of submerged elements in water.

3.2. Potential energy

The total potential energy in the system V is due to conservative forces of buoyancy and gravity which can expressed as:

$$V = V_{1eff} + V_2 \quad (8)$$

$$\text{where } V_{1eff} = \left\{ \sum_{i=1}^{N_p} m_{1i} r_{1i} - \sum_{i=1}^{N_p} f_{1i} r_{1i} \right\} g \cos \theta_1 \quad (9)$$

V_2 consists of the effective potential energy due to top tower and deck. The resulting potential energy may now be expressed as:

$$V_2 = \left\{ \left(\sum_{j=1}^{N_p} m_{2j} - \sum_{j=1}^{N_w} f_{2j} \right) g (L_1 \cos \theta_1 + r_{2j} \cos \theta_2) \right\} + \{ m_{deck} g (L_1 \cos \theta_1 + L_p \cos \theta_2) \} \quad (10)$$

Where f_{2j} is the buoyancy of an element in the top tower.

Now, treating the kinetic and potential energies of the system as per Lagrange's equation, we have:

$$\frac{d}{dt}\left(\frac{\partial T}{\partial \dot{\theta}_1}\right) = (I_{1t} + m_{2t}L_1^2 + m_dL_1^2)\ddot{\theta}_1 + m_{2t}L_1c_2\sin(\theta_2 - \theta_1)\dot{\theta}_1\dot{\theta}_2 - m_{2t}L_1c_2\sin(\theta_2 - \theta_1)\dot{\theta}_2^2 + m_{2t}L_1c_2\cos(\theta_2 - \theta_1)\ddot{\theta}_2 \quad (11)$$

$$\text{where } m_{2t}c_2 = \sum_{j=1}^{N_w} m_{2j}r_{2j} + \sum_{j=1}^{N_w} (am_{2j} + r_{2j}) \quad (12)$$

$$\text{Similarly } \frac{\partial T}{\partial \dot{\theta}_1} = m_{2t}L_1c_2\sin(\theta_2 - \theta_1)\dot{\theta}_1\dot{\theta}_2 \quad (13)$$

$$\frac{\partial V}{\partial \theta_1} = \left[-\sum_{i=1}^{N_p} m_{1i}r_{1i} + \sum_{i=1}^{N_p} f_{1i}r_{1i} + \left(-\sum_{j=1}^{N_p} m_{2j} + \sum_{j=1}^{N_w} f_{2j} - m_dg \right) L_1 \right] g \sin \theta_1 \quad (14)$$

$$\text{or } [(F_1b_1 - W_1c_1) + (F_2 - W_2 - W_d)L_1] \sin \theta_1 \quad (15)$$

Substituting these values in Lagrange's equation leads, first equation of motion as follows:

$$(I_{1t} + m_{2t}L_1^2 + m_dL_1^2)\ddot{\theta}_1 - [m_{2t}c_2L_1\dot{\theta}_2\sin(\theta_2 - \theta_1)]\dot{\theta}_2 + m_{2t}L_1c_2\cos(\theta_2 - \theta_1)\ddot{\theta}_2 + \left[\{(F_1b_1 - W_1c_1) + (F_2 - W_2 - W_d)L_1\} \frac{\sin \theta_1}{\theta_1} \right] \theta_1 = Q_{\theta_1} \quad (16)$$

Treating the same way, various energies with respect to θ_2 , and putting in Lagrange's equation, will yield the second equation of motion as follows:

$$(I_{2t} + I_d + m_dL_p^2)\ddot{\theta}_2 + \{m_{2t}c_2L_1\cos(\theta_2 - \theta_1)\}\ddot{\theta}_1 + \{m_{2t}c_2L_1\dot{\theta}_1\dot{\theta}_2\sin(\theta_2 - \theta_1)\}\dot{\theta}_1 + \left[(F_2b_2 - W_2c_2 - W_dL_p) \frac{\sin \theta_2}{\theta_2} \right] \theta_2 = Q_{\theta_2} \quad (17)$$

where F_1, F_2 are the buoyancy forces in the lower and upper tower; W_1 and W_2 are the weights of bottom and top tower, and C_1, C_2 are the centre of mass of lower and upper tower from respective hinges.

3.3. Generalized forces and their moments

The environmental forces due to wind, waves and currents are categorized as non conservative forces (Simiu and Smith 1996). The combined action of aerodynamic and hydrodynamic forces which constitutes the forcing function is given by:

$$Q = F_a\{u(z), u', \dot{x}\} + F_d(\dot{u}, v_c, \dot{x}) + F_i(\ddot{x}) \quad (18)$$

where $F_a\{u(z), u', \dot{x}\}$ = aerodynamic force, $F_d(\dot{u}, v_c, \dot{x})$ = drag force and $F_i(\ddot{x})$ inertial force.

These loads are defined as:

The wind force per unit of projected area is given by:

$$f_a(y, z, t) = 0.5\rho_a C_p(y, z)[u(z) + u'(y, z, t) - \dot{x}(t)]^2 \quad (19)$$

where $f_a(y, z, t)$ = force per unit area and is a function of space (y, z) and time (t) ; ρ_a = air density; $C_p(y, z)$ pressure coefficient at elevation z and at horizontal coordinate y ; \dot{x} = structural velocity in the horizontal direction parallel to the fluid loading; $u(z)$ = mean wind velocity, and $u'(y, z, t)$ = fluctuating wind velocity.

The total wind induced drag force is then given by:

$$F_a(y, z, t) = \int_{A_a} f_a(y, z, t) dy dz \quad (20)$$

in which A_a is the total projected area of the platform normal to the wind flow.

The drag force is expressed as:

$$F_d = \sum_{i=1}^{N_w} 0.5 C_d \rho_w D_d (\dot{u} + v_c - \dot{x}) |\dot{u} + v_c - \dot{x}| \quad (21)$$

in which ρ_w = mass density of sea water, C_d = drag coefficient, v_c = current velocity, D_d = drag diameter, \dot{u} and \dot{x} are water particle and structural velocity in the direction of fluid flow.

The inertial force is given by:

$$F_i = \sum_{i=1}^{N_w} C_M \rho_w D_i^2 \ddot{u} \quad (22)$$

in which C_M = inertia coefficient, D_i = inertia diameter of i^{th} element and \ddot{u} = wave particle acceleration at the i^{th} element.

4. Super structure model for wind loads

The superstructure details of articulated tower model exposed to wind loads are shown in Fig. 3. The platform comprises of derrick, helideck, boom, mud houses and flare tower, most of which are latticed in nature. Under the influence of wind, the platform superstructure is subjected to aerodynamic drag force in the windward direction. The analysis due to wind forces is carried out by decomposing the wind velocity component into its mean and fluctuating parts. The latticed area of the tower (which is above water) also obstructs wind in surge direction and hence is replaced by their equivalent projected areas.

4.1. Mean wind loading

The mean description of wind field is assumed to be governed either by logarithmic or power law. The logarithmic law is used in the present study and is expressed as:

$$u(z) = u(z_{ref}) = \frac{\ln \frac{z}{z_0}}{\ln \frac{z_{ref}}{z_0}} \quad (23)$$

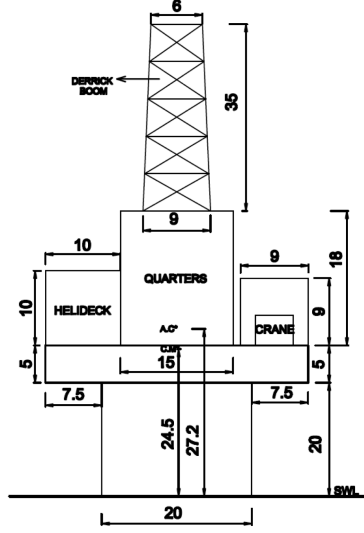


Fig. 3 Super structure detail for wind load assessment (All dimensions are in metres)

where, z_{ref} = Reference elevation above the mean sea level, z_0 = Roughness length which is provided by specifying the value of sea drag coefficient, defined as

$$C_{Dsea} = \left[\frac{K}{\ln(10/z_0)} \right]^2 \quad (24)$$

where ($K = 0.4$) is the Von Karman constant (Kareem 1980).

4.2. Fluctuating wind loading

Single point simulation of wind velocity field is assumed in the present study i.e. the random variation of velocity fluctuations is assumed to be coherent all through the projected area. These fluctuations are simulated by Fourier synthesis of Simiu's spectrum (Simiu and Leigh 1984) and a time series of wind velocity is obtained. Expressions of the Simiu's spectrum $S_u(z, n)$ are:

$$\begin{aligned} \frac{nS_u(z, n)}{U_*^2} &= \{a_1 f + b_1 f^2 + d_1 f^3\} & 0 < f \leq f_m \\ \frac{nS_u(z, n)}{U_*^2} &= \{c_2 + a_2 f + b_2 f^2\} & f_m < f < f_s \\ \frac{nS_u(z, n)}{U_*^2} &= \{0.26 f^{-2/3}\} & f \geq f_s \end{aligned} \quad (25)$$

For various parameters involved in Eq. (25), reference may be made to (Simiu and Leigh 1984).

5. Wind driven waves

A wave pattern is built-up in the sea due to its interaction with the flowing wind. The energy

equation in terms of spectral moment may be expressed as (Gran 1992).

$$0.5 \frac{\rho_a}{g} u(z)^2 \left(1 - \frac{g}{u(z)\Omega}\right)^2 \Omega^4 = -0.5 \rho_w g^2 \frac{1}{\Omega} \frac{\partial \Omega}{\partial x} - \rho_w g \frac{\partial \Omega}{\partial t} \quad (26)$$

where ρ_a , ρ_w is the air and water density; g is the acceleration due to gravity; Ω is the cut-off frequency or weighted mean frequency; $u(z)$ is the nominal wind velocity.

In order to represent the energy of Eq. (26) in terms of a dimensionless basic sea state variable y , put

$$y = \frac{g}{u(z)\Omega} \quad \text{or} \quad \Omega = \frac{g}{u(z)y} \quad (27)$$

The value of y lies between zero and one. For fully developed seas at infinite fetch length, this may be taken as unity. The energy equation Eq. (26) may now be represented by the following differential equation.

$$(1-y)^2 = y^3 \frac{\partial y}{\partial \xi} + y^2 \frac{\partial y}{\partial \tau}, \quad 0 < y < 1, \quad (28)$$

where, ξ is the fetch length; and τ is the wind duration.

The fetch length and wind duration may be obtained by the solution of the above equation as follows:

$$\xi = \frac{y}{1-y} + 3 \ln(1-y) + 2y + \frac{1}{2}y^2 \quad (29)$$

$$\tau = \frac{1}{1-y} + 2 \ln(1-y) - (1-y) \quad (30)$$

The resultant relation between actual time t and duration τ is

$$\tau = 0.60 \times 10^{-4} \frac{g}{u(z)} t \quad (31)$$

For known ξ and τ the sea state y , may be found from the Eqs. (29) and (30). The significant wave height H_s and wave period T_z are then estimated as:

$$H_s = 0.18 \frac{u(z)^2}{g} y^2 \quad (32)$$

$$T_z = \sqrt{2\pi} \frac{u(z)}{g} y \quad (33)$$

6. Simulation of random sea

The synthetic waves corresponding to a particular sea state, represented by a sea surface elevation, are generated by using wave superposition technique suggested by Goda (1970). The linearized small amplitude wave theory allows the summation of velocity potential, wave elevation and water particle kinematics of individual waves to form a random wave made up of a number of components. The generated synthetic random wave is considered to be adequately represented by the summation of K number of sinusoids (harmonics) in random phase. The series representation of

sea surface elevation $\eta(t)$ is given by the equation

$$\eta(t) = \sum_{i=1}^K A_i \cos(k_i x - \omega_i t + \phi_i) \quad (34)$$

$$\text{where } A_i = \sqrt{2[S(\omega_i)\Delta\omega_i]} \quad (35)$$

in which, A_i is the amplitude of the i^{th} component wave, k_i is the wave number of the i^{th} component wave, ω_i is the wave frequency of the i^{th} component wave, ϕ_i is the phase angle of the i^{th} component wave randomly chosen between 0 and 2π , and following the normal distribution, K is the number of wave harmonics considered in the simulation, x is the structural displacement, $S(\omega)$ is the spectral density value of one sided sea surface elevation spectrum at the frequency ω_i .

The selection of frequency ω_i is done such that these frequencies are uncorrelated so that they do not constitute harmonics with each other. First, the range of the frequencies, from the lowest frequency, ω_{\min} to the highest frequency, ω_{\max} is divided into $(k-1)$ sub-ranges with the dividing frequencies constituting a power series of:

$$\omega'_1 = \omega_{\min} + \frac{\omega_{\max} - \omega_{\min}}{k-1} \quad (36)$$

$$\omega'_2 = \omega'_1 C_k \quad (37)$$

$$\omega'_i = \omega'_{i-1} C_k \quad (38)$$

$$\omega'_{k-1} = \omega'_1 C_k^{(k-2)} \quad (39)$$

$$\text{where } C_k = \left(\frac{\omega_{\max}}{\omega'_1}\right)^{\frac{1}{k-2}} \quad (40)$$

Then, the secondary dividing frequencies $\omega''_1, \omega''_2, \omega''_3, \dots, \omega''_{k-1}$ are chosen, at random, in respective sub-ranges. The initial frequency ω''_0 is set equal to ω_{\min} and the last one is $\omega''_k = \omega_{\max}$. The selection is done with the aid of a random-number-generation process program on the computer. Finally the component frequency, ω_i and its bandwidth, $\Delta\omega_i$ is calculated as:

$$\omega_i = 0.5(\omega''_{i-1} + \omega''_i) \quad (41)$$

$$\Delta\omega_i = \omega''_i - \omega''_{i-1} \quad i = 1, 2, 3, \dots, k \quad (42)$$

The above process of random selection of component frequency is repeated for each run of each sea surface elevation spectrum. The random phase angle ϕ_i must be chosen such that the resultant function $\eta(t)$ follows the Gaussian distribution. This has been done with the generation of random numbers normally distributed between 0 and 2π . The computation of sea surface elevation by Eq. (34) is done at discrete intervals of time. The time interval Δt is set to satisfy the condition:

$$\Delta t = \frac{2\pi}{5\omega_{\max}} \quad (43)$$

The value of Δt is chosen as 0.7 second, which is much smaller than what is required from Eq. (43). Though the computation by this method is time consuming, it has the advantage that no restriction is imposed on functional shape of the sea surface elevation spectrum.

7. Solution procedure

The equation of motion Eqs. (16) and (17) is solved by time stepping numerical integration using Newmark- β method. At each time step, an iteration cycle is required to find the solution because the forcing function depends upon the instantaneous structural response. The iteration starts with the instantaneous responses assumed to be the same as those of the previous time station. After solving the equation of motion, obtained values of the responses are used for the next iteration. This procedure is continued until convergence is achieved, i.e. the difference between the two consecutive responses falls below 0.1%.

8. Numerical study

Numerical studies of a double hinged articulated tower in 350 m water depth is carried out to investigate the response due to; (i) wave only and (ii) wind and wave acting together. The details of the idealized tower and environmental characteristics are given in Table 1 and Table 2. Some configuration details such as ballast size, deck location are shown in Fig. 2b. For wind velocity spectrum, mean wind velocities of 10 m/s, 20 m/s and 30 m/s are considered. The exposed area of the tower to wind load is 1288.5 Sq. m. The time domain simulations of the tower response was obtained by selecting a 1200 s (1024 point) wave train ensuring that r.m.s responses attain their steady state values. The wave train was decomposed into a Fourier series and simulated using approximately 50 discrete frequencies. Initial non-stationary phase of the response time histories, which is roughly 10 times the time period of the structure have been ignored. The realized wind velocity spectrum from the simulated wind velocity time history is given in Fig. 4. The P-M spectrum for the sea surface elevation is given in Fig. 5.

Time histories of mid hinge shear response under different wind velocities and correlated waves

Table 1 Geometrical and mechanical characteristics of the tower

Main features	values
Height of bottom tower	240 m
Height of top tower	160 m
Structural mass of top and bottom tower	2.0 E 4 Kg/m
Structural mass of ballast	44840 Kg/m
Deck mass	2.5 E 6 Kg
Fundamental frequency (first and second mode)	0.20 & 0.22 rad/sec
Effective diameter of tower shaft	
For drag	17.0 m
For buoyancy	7.50 m
For inertia and added mass	4.5 m
Effective diameter of Buoyancy chamber	
For drag	20 m
For buoyancy	19.5 m
For inertia and added mass	7.5 m

Table 2 Hydrodynamic and aerodynamic characteristics

Environment	
Water depth	350 m
Mass density of sea water	1025 Kg/m ³
Air density	1.27 Kg/m ³
Current velocity	1.0 m/s
Drag coefficient (C_d)	0.6
Inertia coefficient (C_m)	2.0
wind drag co-efficient (C_D)	0.002
Aerodynamic center above SWL	27.2 m
Total equivalent area for wind load	1288.5 Sq.m
Emil Simiu's wind spectrum constants	
β	6.0
f_s	0.2
f_m	0.07
Roughness length (z_0)	0.001266 m
Length of longitudinal turbulence(L_u)	180 m

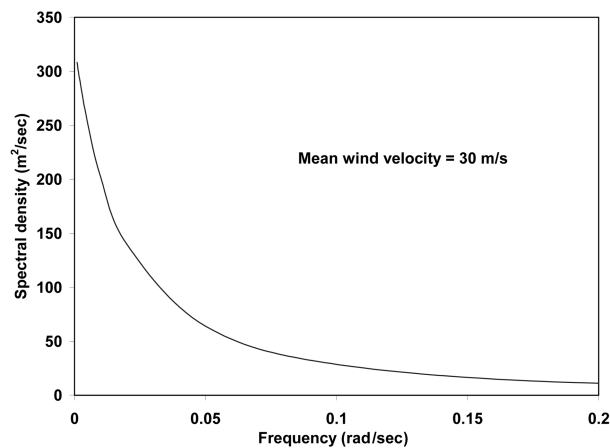


Fig. 4 Emil Simiu spectrum of longitudinal velocity fluctuations

are given in Fig. 6, which shows significant fluctuations or reversal of shear. These fluctuations resulting from the repeated application of wind gusts are responsible for fatigue stresses in the articulation points. Fig. 7 shows the power spectral density function of mid hinge shear under long crested random wave alone, and combined action of wind and wave for a wind velocity of 30 m/s. The highest peak occurs at half the natural frequency, which shows super harmonic resonance. Other peak corresponds to natural frequency of the tower at $\omega_n = 0.2$ rad/sec. In this case, the system responds at lower frequency of the two. That is, at the forcing frequency for the super harmonics. Several other smaller peaks signify nonlinearity in the system. The PSDF clearly

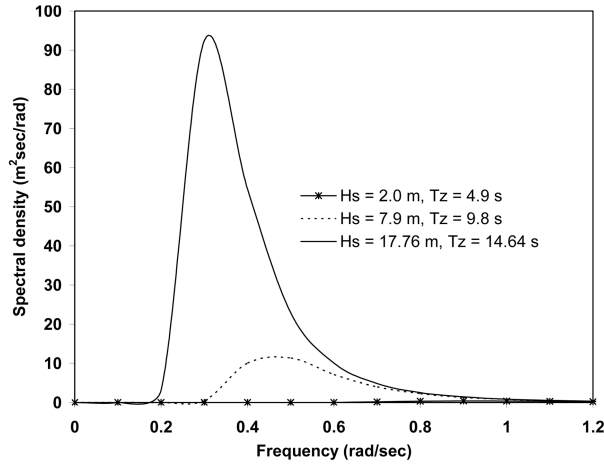


Fig. 5 Pierson-Moskowitz sea surface elevation spectrum

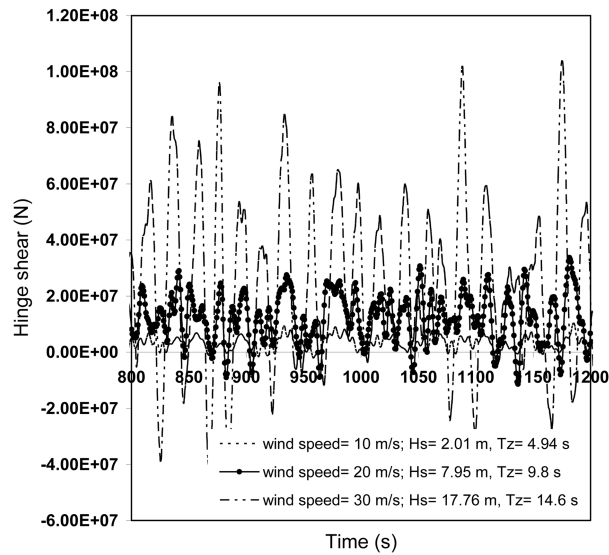


Fig. 6 Mid hinge shear time histories under different wind speeds

indicate that the energy content at the given frequencies is enhanced for the combined effect of wind and waves. The comparative PSDF of base and mid hinge shear is shown in Fig. 8 and is characterized by a prominent peak at a frequency of 0.4 rad/sec. The energy content at this frequency is increased appreciably for mid hinge shear as compared to the base hinge shear.

Fig. 9 shows the PSDF of maximum bending moment of DHAT at a distance of 76.52 m (node no. 25) from mid hinge. The PSDF indicate super harmonic resonance in the system for a wind speed of 20 m/s. As Emil Simiu spectrum has significant energy content at low frequencies; therefore, 20 m/s wind speed contributed appreciably to the bending response. With an increase in the wind speed (30 m/s), wave height and wave period increases nonlinearity in the system leading to the response attenuation.

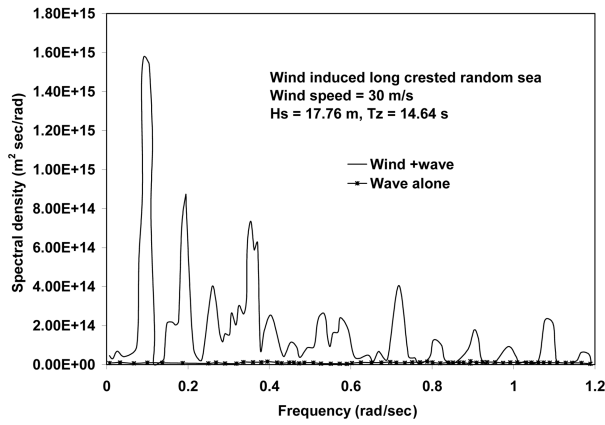


Fig. 7 Effect of wind on PSDF of mid hinge shear of DHAT

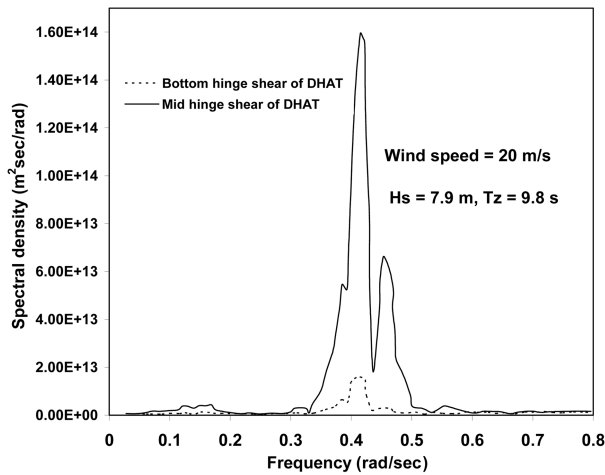


Fig. 8 Comparative PSDF of hinge shear of DHAT under wind loading

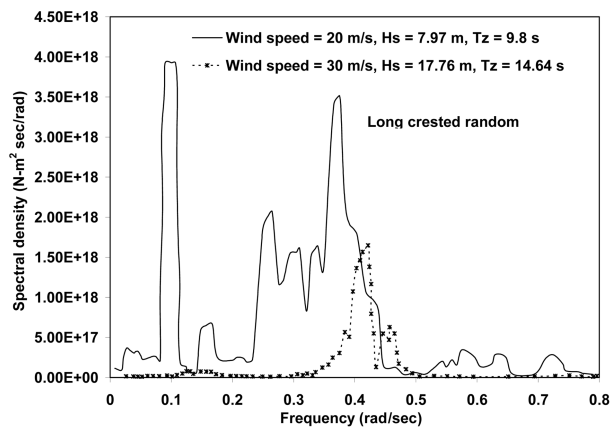


Fig. 9 Comparative PSDF of maximum B.M of DHAT under wind loading

Fig. 10 shows the comparative time history of deck displacement under various wind velocities for the stabilized sea states. It is observed that mean wind displaces the tower off the mean position where it vibrates under wind gustiness. The corresponding power spectra in Fig. 11 show a low frequency super harmonic resonance. Another peak appears close to the structural fundamental frequency. The third prominent peak occurs in the vicinity of forcing frequency of wind driven waves.

Due to stochastic nature of the responses, the results are also presented statistically in Tables 3 to 5. Important statistics such as maxima, minima, RMS, mean and standard deviation are reported. Table

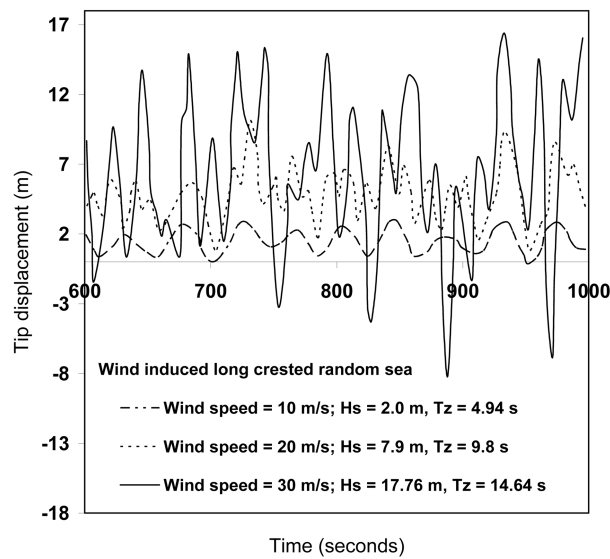


Fig. 10 Time history of tip displacement under different wind speeds

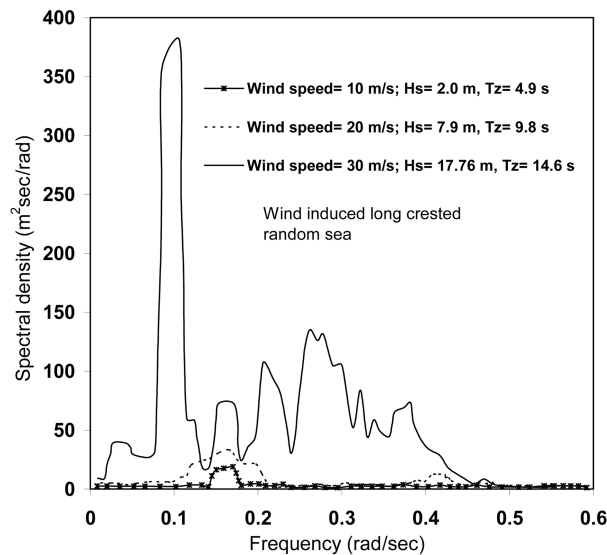


Fig. 11 Comparative PSDF of tip displacement under various wind speeds

Table 3 Hinge angle response of DHAT under different ocean environments

Sea environment		Statistics	θ_1 (radians)		θ_2 (radians)	
Wind velocity	Wind driven waves		Wave alone	Wave +wind	Wave alone	Wave +wind
10 m/s	$H_s = 2.015$ m $T_z = 4.94$ sec	Max.	7.31E4	4.72E-3	1.65E-3	1.17E-2
		Min.	-7.9E-4	-1.24E-3	-1.61E-3	4.98E-4
		RMS	3.70E-4	2.05E-3	7.95E-4	6.85E-3
		Mean	-1.2E-5	1.52E-3	-2.70E-5	5.75E-3
		S.D	3.70E-4	1.37E-3	7.95E-4	3.18E-3
30 m/s	$H_s = 17.76$ m $T_z = 14.64$ sec	Max.	1.35E-2	2.57E-2	6.12E-2	1.06E-1
		Min.	-5.53E-2	-2.78E2	-1.48E-1	-5.69E-2
		RMS	1.43E-2	1.04E-2	4.11E-2	4.46E-2
		Mean	1.07E-2	3.84E-3	-2.47E-2	3.08E-2
		S.D	1.01E-2	9.70E-3	3.29E-2	3.22E-2

Table 4 Hinge shear response of DHAT under different ocean environments

Sea environment		Statistics	Base hinge shear (N)		Mid hinge shear (N)	
Wind velocity	Wind driven waves		Wave alone	Wave +wind	Wave alone	Wave +wind
10 m/s	$H_s = 2.015$ m $T_z = 4.94$ sec	Max.	3.10E5	1.76E5	2.54E5	-3.55E4
		Min.	-3.0E5	-8.5E5	-2.4E5	-1.58E6
		RMS	1.00E5	3.90E5	9.00E4	8.367E5
		Mean	2.71E3	-3.3E5	4.70E3	-7.61E5
		S.D	1.00E5	1.96E5	8.98E4	3.465E5
30 m/s	$H_s = 17.76$ m $T_z = 14.64$ sec	Max.	1.65E7	9.58E7	2.94E8	1.65E8
		Min.	-4.7E6	-7.8E6	-8.8E6	-1.4E7
		RMS	1.16E7	9.02E6	2.99E7	2.24E7
		Mean	4.91E6	1.29E6	2.13E7	1.28E7
		S.D	1.05E7	8.93E6	2.10E7	1.83E7

3 shows the effect of wind on hinge angles of DHAT. The maximum hinge angle for upper tower θ_2 is more as compared to the lower tower θ_1 for both the loading environments. The RMS values of upper hinge angle under wind and waves increases 8.6 times over wave alone when wind velocity is 10 m/s, whereas for wind velocity of 30 m/s, a marginal increase in the RMS hinge angle is observed. It is also seen that the dynamic effect of wind assumes significance at lower wind velocity when the wave's significant energy contents are far away from it. The standard deviation for wave becomes closer to the standard deviation obtained for combined wind and wave when the wind velocity is 30 m/s.

Table 4 shows the effect of wind on the hinge shear response of the tower. Hinge shear is an important parameter due to reversal of stresses, which cause fatigue at the articulation points. These stresses are subsequently used for the reliability analyses. It is seen that mid hinge shear values are

Table 5 Bending moment response of lower and upper shaft of DHAT (N m)

Sea environment		Statistics	At 114.78 m from base hinge		At 76.52 m from mid hinge	
Wind velocity	Wind driven waves		Wave alone	Wave +wind	Wave alone	Wave +wind
10 m/s	$H_s = 2.015$ m $T_z = 4.94$ sec	Max.	1.66E7	7.03E6	4.48E7	2.31E7
		Min.	-1.7E7	-2.0E8	-4.6E7	-3.0E7
		RMS	5.69E6	1.07E7	1.51E6	1.03E7
		Mean	9.75E4	-9.6E7	5.43E6	-3.5E6
		S.D	5.69E6	4.77E7	1.51E6	9.69E6
30 m/s	$H_s = 17.76$ m $T_z = 14.64$ sec	Max.	3.94E9	1.13E9	2.1E10	2.20E9
		Min.	-2.8E8	-1.9E8	1.35E9	-3.2E8
		RMS	3.12E8	1.25E8	1.65E9	2.25E8
		Mean	1.45E8	-1.2E8	8.21E8	6.99E7
		S.D	2.76E8	1.25E8	1.43E9	2.46E8

higher as compared to base hinge shear as a heavy deck is placed on the top tower. An increase in wind speed from 10 m/s to 30 m/s results in a 17-fold increase in the mean value of hinge shear response (mid hinge shear) under combined effect of wind and wave, whereas for base hinge shear, a four-fold increase in the mean value is noticed for the same loading.

Table 5 shows the statistics of the bending moment response. It is observed that the standard deviation for both the upper and lower shafts of DHAT decreases when the combined effect of wind and wave force is considered.

9. Conclusions

Following conclusions are drawn from the present study.

1. Participation of wind induced forces in the response is governed by the size of wind driven waves. High wind speed generates larger waves (higher H_s and T_z), the wind participation to the response is marginal due to the wave significant frequency becoming smaller and in the vicinity of wind frequency and thereby suppressing the response caused by the wind. Whereas, in case of low mean wind speed, the contribution of wind forces is significant, because the significant wave frequency becomes higher and moves away from the wind frequency.
2. Wind loads may increase the static offset significantly so that the tower behaviour may become nonlinear. In the presence of waves together with wind, drag force causes sub and super harmonic response, which gives significantly different response than due to wave alone loading.
3. The response of articulated tower to wind is primarily in resonant mode, emphasizing the significance of a reliable estimate of damping. Due to a small source of damping, both from structural and hydrodynamic sources, surge motion even at low wind speeds has the potential of introducing problems from a fatigue viewpoint.
4. For fatigue reliability evaluation, central hinge is more critical in comparison to base hinge because of significant energy content at the central hinge.

Nomenclature

KE	= kinetic energy
PE	= potential energy
θ_1, θ_2	= rotation angle of bottom and top tower about the respective hinges
$M\theta_1, M\theta_2$	= generalized moment due to non conservative forces w.r.t θ_1 and θ_2
$\dot{\theta}_1, \dot{\theta}_2$	= angular velocity of bottom and top tower
$\ddot{\theta}_1, \ddot{\theta}_2$	= angular acceleration of bottom and top tower
I_1^*, I_2^*	= moment of inertia of bottom and top tower including added mass
I_d	= moment of inertia of the platform deck
m_d	= mass of deck
L_1, L_2	= length of bottom and top tower respectively
C_1	= centre of mass of lower tower from bottom hinge
F_1, F_2	= buoyancy forces in the lower and upper tower respectively
W_2^*	= weight of top tower
M_2	= mass of top tower including added mass
C_2	= centre of mass of upper tower from top hinge
ρ_a	= mass density of air
ρ_w	= mass density of water
$C_p(y,z)$	= pressure coefficient at elevation z and at horizontal coordinate y
$u(z)$	= mean wind velocity
$u'(y,z,t)$	= fluctuating wind velocity
$\dot{x}(t)$	= structural velocity in the direction of fluid motion
A_a	= projected area of the platform
z_{ref}	= reference elevation
z_o	= roughness length
K	= Von Karman constant
$S_u(z,n_i)$	= spectrum of fluctuating wind energy
U_*	= friction velocity
f	= non dimensional frequency
f_m, f_s	= Emil Simiu's constants
g	= acceleration due to gravity
Ω	= cut-off frequency
ξ	= fetch length
τ	= wind duration
H_s, T_z	= wave height and wave period
ϕ_i	= phase angle
C_a	= coefficient of wind drag
A_i	= amplitude of the i^{th} component wave
k_i	= wave number of the i^{th} component wave
ω_i	= wave frequency of the i^{th} component wave
ϕ_i	= phase angle of the i^{th} component wave
K	= number of wave harmonics considered in the simulation
$S(\omega)$	= spectral density value of one sided sea surface elevation spectrum
ω_{min}	= lowest frequency

ω_{\max}	= highest frequency
ω_i	= component frequency
$\Delta\omega_i$	= bandwidth

References

- Ahmad, S. (1995), "Stochastic TLP response under long crested random sea", *J. Comput. Struct.*, **61**(6), 975-993.
- Ahmad, S. and Islam, N. (2001), "Wind induced response of articulated tower", *Proc. of the Int. Conf. in Ocean Engineering, IIT Madras, India*, 21-27.
- Ahmed, S., Islam, N. and Ali, A. (1997), "Wind induced response of tension leg Platform", *J. Wind Eng. Ind. Aerod.*, **72**, 1-16.
- Bar-Avi, P. and Benaroya, H. (1995), "Response of an articulated tower to loads due to wave slamming, wind and Coriolis acceleration", *Proc. of 36th AIAA/ASME/ASCE/ASC; Structural Dynamics and Material Conf.*, 257-265.
- Bar-Avi, P. and Benaroya, H. (1997), "Stochastic response of a two DOF articulated tower", *Int. J. Nonlin. Mech.*, **32**(4), 639-655.
- Bisht, R.S. and Jain, A.K. (1998), "Wind and wave induced behaviour of offshore guyed tower platforms", *Ocean Eng.*, **25**(7), 501-919.
- Chakrabarti, S.K. and Cotter, D.C. (1978), "Analysis of tower tanker system", *Proc. 10th Offshore Technology Conf.*, **3**(3202), 1301-1310.
- Datta, T.K. and Jain, A.K. (1990), "Response of articulated tower platforms to random wind and wave forces", *Comput. Struct.*, **34**(1), 137-144.
- Deleuil, G.E., Durgeat, E.A. and Doris, C.G. (1987), "Long term response of articulated towers to wind waves and current", *Offshore Technology Conf.*, 3105, Huston, 465-472.
- Gran, S. (1992), *A Course in Ocean Engineering*, Elsevier Science publication.
- Hanna, S.Y., Karsan, D.I. and Yeung, J.Y. (1988), "Dynamic response of a compliant tower with multiple articulations", *Proc. of Int. Conf. on Offshore Mechanics and Arctic Engineering Symposium*, **1**, 257-269.
- Hevacioglu, I. and Incecik, A. (1988), "Dynamic analysis of coupled articulated tower and floating production system", *Proc. of the 7th OMAE Conf.*, 279-287.
- Islam, N. and Ahmad, S. (2003), "Random wave response of double pendulum articulated offshore tower", *Proc. of the 22nd Int. Conf. on Offshore Mechanics and Arctic Engineering*, Cancun, Mexico, **1**, 489-498.
- Islam, N. and Ahmad, S. (2007), "Reliability of articulated tower joint against random base shear", *Struct. Eng. Mech.*, **27**(1), 33-48.
- Kareem, A. (1980), "Dynamic effects of wind on offshore structures", *Proc. of the 12th Annual Offshore Technology Conf.*, Houston, Texas, 235-242.
- Kim, C.H. and Luh, P.A. (1982), "Prediction of pitching motions and loads articulated loading platform in waves", *Proc. of the 14th OTC Conf.*, 4247, Texas May 3-6, 205-213.
- Kuchnicki, S.N. and Benaroya, H. (2002), "A Parametric Study of a flexible ocean tower", *Chaos, Solitons Fract.*, **14**, 183-201.
- McNamara, J.F. and Lane, M. (1984), "Practical modeling for articulated risers and loading columns", *J. Energ. Resour.-ASME*, **106**, 444-450.
- Simiu, E. and Stefan, D. L. (1984), "Turbulent wind and TLP surge", *J. Struct. Eng.*, **110**(4), 785-802.
- Smith, C.E. and Simiu, E. (1996), *Wind effects on compliant offshore structures*, The American Society of Civil Engineers, New York.
- Zaheer, M.M. and Islam, N. (2008), "Fluctuating wind induced response of double hinged articulated loading platform", *Proc. of the 27th OMAE Conf.*, 57723, Estoril, Portugal.
- Zaheer, M.M. and Islam, N. (2008), "Aerodynamic response of articulated towers: State-of-the-art", *Wind Struct.*, **11**(2), 97-120.
- Zeng, X., Liu, Y., Shen, X. and Wu, Y. (2006), "Nonlinear dynamic response of tension leg platform", *Proc. of the 16th ISOPE Conf.*, 94-100.